A Real-time Patient-Specific Sleeping Posture Recognition System using Pressure Sensitive Conductive Sheet and Transfer Learning

Qisong Hu, *Student Member, IEEE*, Xiaochen Tang, *Student Member, IEEE*, and Wei Tang, *Member, IEEE*

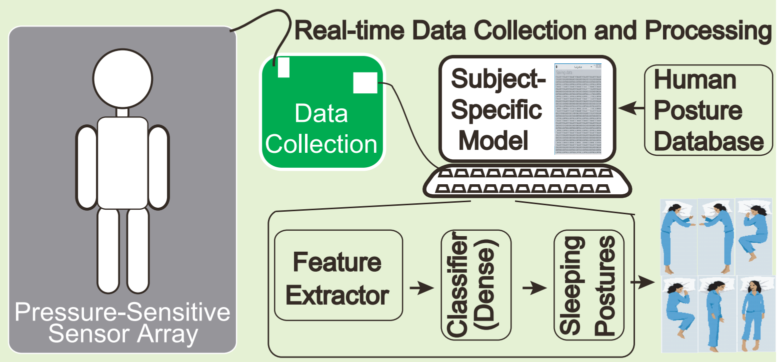

***Abstract*—Sleeping is an indispensable activity of human beings. Sleeping postures have a significant effect on sleeping quality and health. A real-time low-cost sleeping posture recognition system with high privacy and good user experience is desired. In this paper, we propose a sleeping posture recognition system based on a low-cost pressure sensor array which consists of conductive fabric and conductive wires. The sensor array is deployed as a bedsheet with 32 rows and 32 columns resulting in 1024 nodes. An Arduino Nano performs data collection using a 10-bit Analog to Digital Converter (ADC). The sampling rate of the overall sensor array is 0.4 frame/sec. Six health-related sleeping postures of five participants can be recognized by a shallow Convolutional Neural Network (CNN) deployed on a Personal Computer (PC). The system accuracy achieved 84.80% using the standard training-test method and 91.24% using the transfer learning-based subject-specific method. The real-time processing speed achieved 434 us/frame.**

***Index Terms*—Artificial Neural Network, Realtime Classification, Sensor Array, Smart Bed, Sleeping Postures ,**

I. Introduction

WEARABLE biosensors [1]–[7] are widely used to monitor human status and postures [8]–[13]. Sleep is one of the most important postures as a vital activity of human beings and plays an important role in recovery and survival [14]. People sleep about 8 hours a day for average which is one-third of their life [15]. Sleeping postures have been proven to be related to human health. The bad postures can cause health issues or worsen the existing diseases, which may increase the death risk. For example, the supine position is significantly associated with apneas, which affects up to 4 percent of middle-aged adults [16]. Besides, for the late pregnancy women, if a supine posture is adopted, the pregnant uterus may impact the aorta and inferior vena cava [17]. A greater visual field (VF) loss may be associated with the lateral decubitus postures [18]. Sleeping with one posture for a long time may also cause or worsen the pressure ulcer. The pressure ulcer can be avoided by using different sleep postures [19]. Thus, continuously monitoring the sleeping postures is important for people who have been affected by related health problems. However, the global nursing shortage is impacting the health system around the world negatively [20]. Therefore, automatic systems that have the capability of continuously monitoring patient sleeping postures are expected.

To recognize and monitor the sleeping postures of human beings, many works have been proposed. For instance, accelerometers based monitoring systems [21]–[23] were presented. However, the sensors (accelerometers) must be attached to the user's body, which brings a bad user experience. Another type of monitoring systems using vision devices [24]–[26] includes the method of using visible light cameras, Infrared cameras, Kinect cameras. Besides, a commercial product [27] using the short pulse of radio waves has been designed. However, the performance of these vision-based monitoring and the short pulse of radio waves systems can be easily impacted by the background, occlusion, and environmental change, which may also make the user uncomfortable for privacy issues. More privacy issues come if the systems transmit the recorded data via the internet for cloud processing, which may cause information leakage. Thus, building sleep posture monitoring systems using pressure sensors became a hot research topic.

Several important works of sleep monitoring systems using

Manuscript received August 30, 2020; revised XXX XX, 2020; accepted XXX XX, 2020. Date of publication XXX XX, 2020; date of current version XXX XX, 2020. This work was supported by the United States National Science Foundation under Grant ECCS-1652944 and ECCS-2015573.

The authors are with the Klipsch School of Electrical and Computer Engineering, New Mexico State University, Las Cruces, NM 88003 USA (Corresponding author: Wei Tang, e-mail: wtang@nmsu.edu).

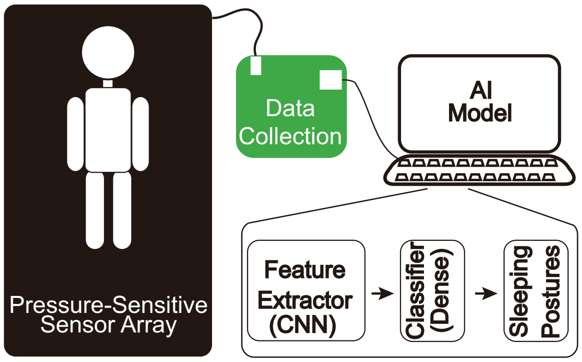

Fig. 1: Block diagram of the sleeping posture recognition system.

pressure sensors have been reported in recent years [28]–[44]. These systems usually employ a sensor array to detect the pressure distribution on the bedsheet. The pressure distribution map is then processed as images using feature extraction and learning methods to classify sleeping postures. The popular processing methods include the k-nearest neighbor algorithm (KNN), Convolutional Neural Network (CNN), and earth movers distance (EMD). The main shortcomings of the current system come from cost, flexibility, and real-time processing capability. For example, the Force-Sensitive Resistance (FSR) units can be expensive if a large array is requested. This limits the flexibility of such systems for home care and travel. Another challenge is that the data processing procedure is usually separated from data collection, therefore, real-time classification can not be achieved. Moreover, current systems haven't been reporting subject-specific inference methods. Since individual patients may have different conditions, i.e., body mass indexes, the pressure distribution may vary. A subject-specific inference system may better fit the personalized health system.

To overcome the above-mentioned challenges of current systems, a low-cost real-time local sleeping posture recognition system with low computational complexity is desired. In this paper, we presented a sleeping posture recognition system built using pressure-sensitive conductive sheets and conductive threads with an amount of 1024 (32x32) nodes. The sensor array, including the conductive sheets, is shaped as a bedsheet with a size of 90cm x 180cm. A data collection module was built on a Printed Circuit Board (PCB) board with an Arduino Nano as the microcontroller. The 10-bit Analog to Digital Convertor (ADC) in the Arduino Nano samples the data and sends the data to a PC using Universal Asynchronous Receiver/Transmitter (UART) by a Universal Serial Bus (USB) cable. A CNN model is trained with data from MPII Human Pose Dataset [45] and data collected from 5 participants (3 male and 2 female). Applied Transfer Learning (TL), the system achieves the goals of obtaining high performance and low complexity computation overhead. Transfer learning is realized using Tensorflow 2.0. The accuracy of subject-specific method achieves 91.24% $\pm$ 7.37% with loss as 0.377 $\pm$ 0.245 and the processing speed as 367.8 $\pm$ 37.12 μs/sample.

The main contribution of the system includes (1) providing a low complexity low-cost hardware sensor using conductive threads and pressure-sensitive conductive sheets. The cost analysis is further discussed in Section V; (2) introducing the machine-learning algorithm with transfer learning using the MPII database for subject-specific classification to compensate the accuracy loss from the low-cost hardware sensors for real-time processing; (3) implementing the real-time operation that achieved more than 2 frames/second. The main contribution of this paper focuses on system integration with transfer learning.

The rest of this paper is organized as follows. In Section II, the details of the design of this system and sensors, including concepts and structures, are introduced. In Section III and IV, the experimental setup and results are shown. Section V discusses the advantage and limitations of the proposed system. Section VI concludes this paper.

II. System and Sensor Design

A brief diagram of the system is shown in Fig 1. The sleeping posture recognition system is made of a pressure-sensitive sensory array, a data collection module, and a CNN implemented on a PC. The data collection module samples the voltage of the sensor array which is implemented as the bedsheet. The data collection module sends the data to the PC using a USB cable with the UART protocol. The CNN on the PC processes the collected data using a Python program to classify the sleeping posture from the subjects. A total of six health-related sleeping postures were selected which is shown in Fig 2. The selected sleeping postures are (a) Right Yearner, (b) Left Yearner, (c) Left Foetus, (d) Right Foetus, (e) Log, and (f) Supine. The target sleeping postures are selected as typical postures which are also widely used in previous literature studying the sleeping posture recognition [31], [41]. Fig 2 also illustrates typical data collected from the sensor array as images. The overall data come from two sources. The first source is the images of the human body from the MPII dataset, while another source is the data collected from the subjects. We collect shallow data from the subjects and use transfer learning to meet the target of classification accuracy and generalization.

A. Sensor Array

The sensor array contains 1024 pressure sensors with 32 rows and 32 columns made by pressure-sensitive sheets and conductive threads. The structure of the sensor array is shown in Fig. 3. The pressure-sensitive sheet is made of conductive material also known as “Velostat” or “Linqstat”. Each sheet patch is 11”x11” (28cm x 28cm) with a thickness of 4mil (0.1mm). The sheet has variable resistance between its two sides when implementing different pressure across the sheet. Higher pressure results in a lower resistance between the two sides. When the pressure is removed, the resistance recovers back to its original value. Therefore, we use stainless conductive threads to form the sensor, which is the same method as employed in [46]. The crosses of the row thread and the column thread on different sides provide pressure information of the crossing points. We attached 32 conductive stainless threads to the top surface of the pressure-sensitive

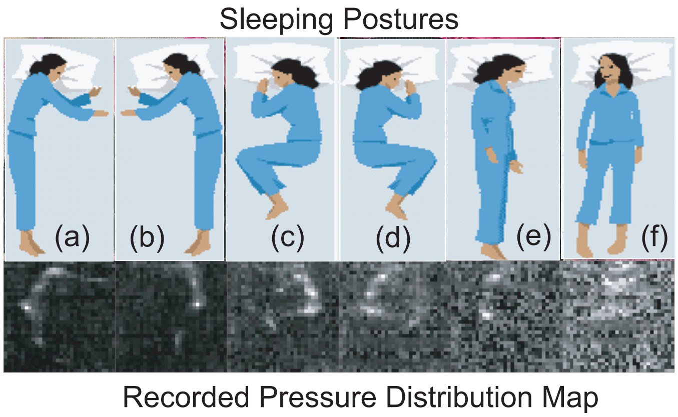

Fig. 2: Six selected sleeping postures and the typical pressure map of each posture.

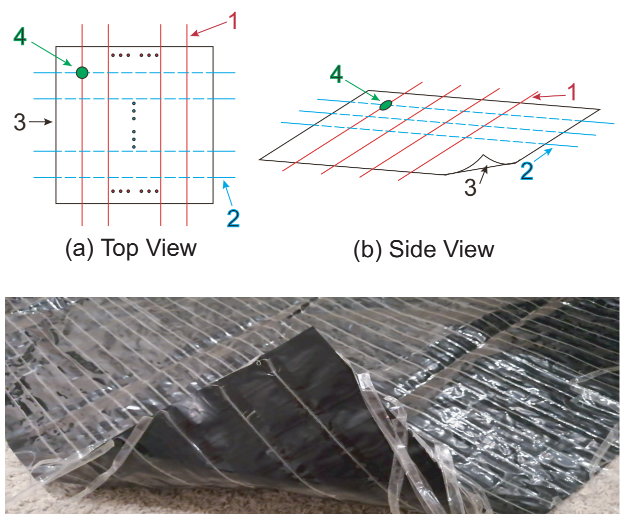

(c) Smart-bed Sheet Sensor

Fig. 3: Structure of the pressure sensors.

sheet with tapes as rows while another 32 conductive stainless threads were attached to the bottom surface of the pressure-sensitive sheet as columns, which is perpendicular to the top threads. This avoids the extra wire layers in the high-thickness sandwich structure like [33], [34]. The cross point between the top thread and the bottom thread forms the sensor nodes. The overall sheet is connected by 18 (3x6) small sheet whose size is 31cm by 31cm. The overall sheet is size is 0.9 m by 1.8m. The distance between two neighboring sensor nodes is 2.72cm horizontally and 5.45cm vertically. After assembly, the measured original resistance between the two sides of a sensor node is about 20k ohms. To measure the resistance of each sensor node, each time one top thread and one bottom thread are selected. The resistance of the cross node between the two threads is then measured by a voltage divider and sampled by an Analog to Digital Converter.

We measured the resistance across the conductive sheet with different scale weights on top of the sheet. The resistance varies from about 23k Ohm to 3.5k Ohm while the weight on top of the sheet increases from 10g to 150g. The minimum detectable weight (sensitivity) is 10g. The experiment result is shown in Fig. 4.

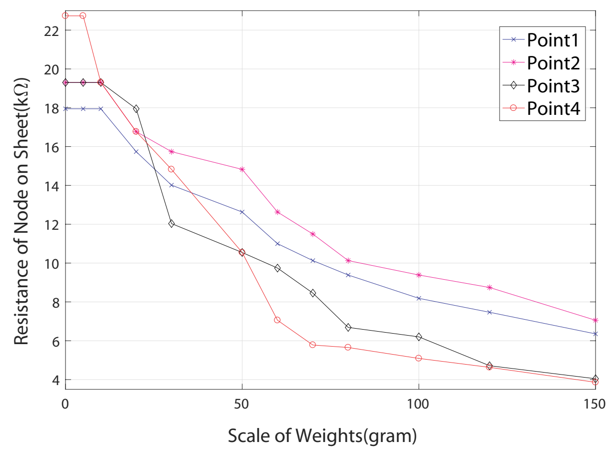

Fig. 4: Resistance across the conductive sheet with different weight at four points on the sheet.

B. Ethical approval and Participant Selection

Ethical approval for this work has been granted by the Office of Research Compliance of New Mexico State University with project ID 18962. Each participant has been explained the key information and has signed the Informed Consent Form. The selected participants consist of 5 healthy young people (2 female and 3 male) with the age ranging from 26 to 31, mean $\pm$ standard deviation as 29.2 $\pm$ 1.5; weight ranging from 52 to 80 kg, mean $\pm$ standard deviation as 64.20 $\pm$ 11.5 kg; height ranging from 162 to 177 cm, mean $\pm$ standard deviation as 168.8 $\pm$ 5.8 cm. The participants were asked to lay on the sleeping monitoring system with 6 specific postures mentioned above. Each participant stays in one posture for 5 minutes. The identification of each participant is anonymously coded and stored in a classified file.

C. Data Collection and Storage

The data collection module is on a custom design PCB that hosts the components of the Arduino Nano board, 4-to-16 decoders, analog single pole double throw switches (SPDT), and active voltage dividers. The data collection module connects the threads on the bedsheet. The threads on the top of the bedsheet are connected to the output pins of SPDT by jumping wires. The threads on the bottom of the bedsheet are connected to the input pins of the voltage dividers. The Arduino Nano board contains both the Microcontroller Unit (MCU) and ADC to control the scanning of the sensor array and sample the voltage of the voltage divider each time when a sensor node is selected for resistance measurement. This is done by the active voltage divider, which can adjust the sampled voltage into the range from 2.5V to 5V. This voltage range fits both the power supply range and the ADC input range. The 10-bit ADC on the Arduino Nano board converts the output signal of the voltage divider into digital data.

The sensors are shaped as a 32x32 array on the conductive sheet. We collected the data by scanning the nodes one by one.

At the beginning of the scan, a string of “frame start” is sent as the starting flag. Then a conductive row thread is activated by switching from the reference voltage to the ground. Because another end of this sensor has been connected to the input of an inverting amplifier, which works as a voltage divider, the change of the resistance of one node can be transferred to the voltage signal. Next, a conductive column thread is selected to be read. The output port of each voltage divider is connected to one input port of the analog switch. By changing the analog switch to the corresponding column, we can select 32 different nodes in the row. The scanning repeats 32 times for rows. 32 columns of thread are selected to be read respectively. At the end of each scanning, a string of ”frame complete” is sent as the ending flag.

The initialization of the system is operated at the beginning of the data collection. The initialization contains the scanning of all the nodes. The data collected during initialization can be used to check the status of each node. After initialization, a ready signal is sent from the MCU to the PC. Once data collection starts, a command is sent to the MCU and the continuous scanning operates. If a stop command is sent from the PC to the MCU, the system still collects the data for the remaining frames. This can guarantee a frame of data to be collected completely. With the scanning method applied in this work, only one row of sensors is active, which brings low power consumption of the sensor even when the whole system is working during continuous monitoring.

The collected data are sent and stored on a PC using a mini USB cable. The communication is based on the UART protocol with a baud rate of 115200. The sampling rate of the system is 0.4 frame per second which means 2.44ms/node. The PC processes the incoming data using an Intel i7 CPU and Python program. Numpy and Tensorflow 2.0 libraries were used to process the raw data, such as the operation of normalization, reshape, and dimension transfer.

D. Signal Processing using Machine Learning

Machine learning has been applied to the sleep monitoring system, such as the K-nearest neighborhood (KNN) method [32], [37], Artificial Neuron Network (ANN) method [28], and Deep Neural Network (DNN) method [29], [31]. Machine learning methods achieve higher accuracy in posture classification compared to analytical methods. In this work, we applied the Convolutional Neuron Network. The CNN sleeping posture recognition as illustrated in Fig. 5, which shows the dimension of the input and output of each layer. The input of CNN is the data from the sensor array with a size of 1024 (32x32). The output of the CNN is the 6-bit one-hot binary code which represents the sleeping posture predicted by the model. The model has 4 layers. The first layer and the second layer are convolutional layers with max pooling. The filters of these two layers are 3x3x32 and 1x1x32. Zero padding is applied to obtain information from all the data, which can correspond to the convolution operation whose center is the specific data. By doing so, the output of the convolution operation, which is the feature map, has the same size as the input data. The last two layers are the fully connected layers with 32 and 6 nodes, respectively. The first two layers use the activation function of the rectified linear unit (ReLU), and the third layer uses the activation function as Hyperbolic tangent. The first two layers play the role of feature extractors while the last two layers act as classifiers.

1) Transfer Learning: Transfer learning is applied in the system to improve classification accuracy [47]. Transfer learning is introduced to alleviate the problem of overfitting during model training due to shallow data. The data we collected contains the feature of the body shapes of participants, which is similar to the feature of the data from the MPII dataset. Transfer learning can realize knowledge transfer by training a model to extract a similar feature with the MPII dataset. Then we can obtain shallow fully connect layers that were trained just for classification to alleviate the overfitting problem. Transfer learning is a popular way to train a model with shallow data. The system applies transfer learning using data from both the recorded data and the database. The recorded data were collected from the 5 participants, which contains a total of 3005 frames and each frame has 1024 nodes. Data from each node is stored as 32-bit floating numbers. Another source of transfer learning comes from 7000 images in the MPII database. We first train the model using images from the database. To get balanced data, we cut the images from the MPII database so that 50% of the images contain human body shapes while the other 50% of the images do not contain human body shapes. The images with humans are labeled as the binary number “10”, while the images without a human are labeled as “01”. A 4-layer CNN was selected as the model and trained as a classifier. The first two layers are 2 2-Dimension convolutional layer. Then 2 fully connected layers attached to the first two layers. The first layer has 32 filters with a shape of 3x3 and a 2-Dimensional Maxpooling operation. The second layer has 32 filters with shape as 1x1 and a 2-Dimensional Maxpooling operation as well. The maxpooling operation in these two layers is with a size of 2x2 and the stride as 2.

The activation function for the first two layers is ReLU. To utilize all the information, zero padding is applied to these two layers, so that the size of feature maps of the convolution operation is the same as the input. After flattening all the output of the second layer, a fully connected layer is attached. This layer has 256 nodes with activation function as Hyperbolic tangent which can utilize the value of both positive and negative numbers. The last layer in the model for the MPII dataset is another fully connected layer, which works as the output of the model. Dropout operation is applied to all the layers except the last layer to avoid overfitting, and the parameters are all set at 0.2 for these three layers. The numbers of filters and nodes are selected as the power of 2. Cross-validation was used to choose the optimal combination. The fully connected layers of the model trained with the dataset were removed after training. The rest of this model then acts as the feature extractor in the new model for transfer learning. All 32 filters of the first layers are shown in Fig.6

In the second step of transfer learning, we use the recorded data to finalize the model parameters. The recorded data is divided into a training set (70%) and a test set (20%). Two fully connected layers were attached to the output of the model

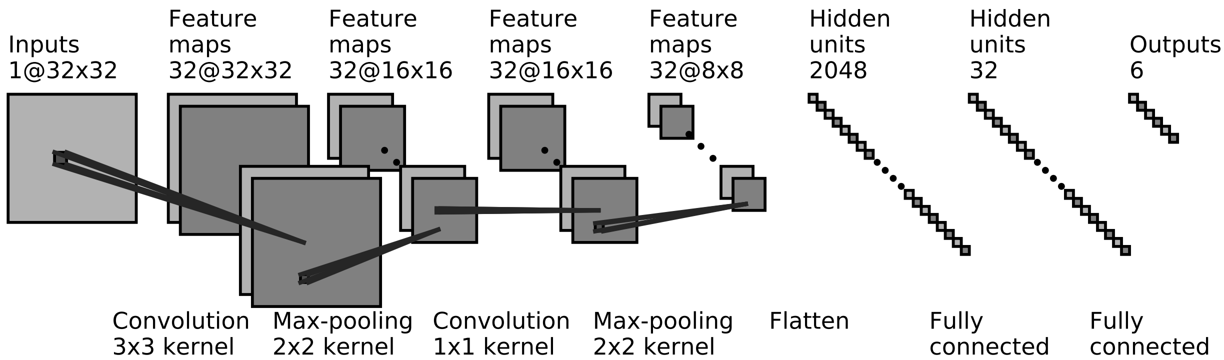

Fig. 5: Structure of the CNN applied transfer learning

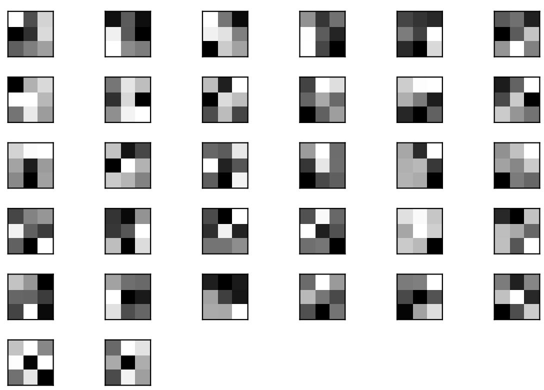

Fig. 6: The filters of the first layer of CNN. Each filter has the size of 3x3. The total amount of filters is 32.

trained with data from the dataset. The first fully connected layer has 32 nodes with the activation function as Hyperbolic tangent. The last layer has 6 nodes where the number is the same as the number of postures to be classified. Dropout operation is applied to the first fully connected layer with a parameter as 0.5. The input of the new model is the frame of pressure image of 1024 (32x32) nodes. The output of the new model is a 6-bit one-hot binary code that corresponds to specific sleeping postures.

2) Histogram of Oriented Gradients: Histogram of Oriented Gradients (HOG) is an attractive and effective way to extract features for object detection, especially for the edge of objects in the images or pressure maps. Applying filters in horizontal and vertical directions, the HOG result can be set as groups by setting the size of a cell and the number of the cells in one block. The number of orientation bins is another parameter that can affect the granularity of the HOG. HOG often combines with Support Vector Machine (SVM) to perform classification, which is also applied in this work to compare with CNN and transfer learning methods. In our systems, the size of each cell is 8x8, and only 1 cell in a block. The number of orientation bins is 4, which can be easily realized with 4 different combinations of result signs of the convolution operation between data and two filters. Thus, the dimension of feature vectors for each frame is 64 (4x4x4). The feature vectors are calculated and normalized to the range between -1 and 1. 70% of data is used to train the SVM and another 30% of data is used to test the model. The typical feature vectors for 6 selected sleeping postures are shown in Fig.7.

III. Experimental Setup

During the experiment, each participant laid on the smart bedsheet of the sensor array. The sensor array, the data collection module, and a PC were connected with jumping wires and a USB cable. The data collection module was powered by two USB cables. One cable was between the PC and Arduino Nano board, which can be used as both power supply and data transmission. Another USB cable was between the PC and power supply pins of the other chips on the data collection module board. Data from each node was sampled by the Arduino Nano and transmitted to the PC. Then, the data were processed by Python programs and stored in the hard drive. The integrated sleep posture recognition system is shown in Fig.8.

A. Data Processing

The data for this work consisted of two parts. One part was the images that include human from the MPII dataset. Another part was the data collected from the five participants. The positions of four corners about bounding boxes that include human bodies were labeled by the MPHB dataset which is a subset of the MPII dataset. 3500 boxes with human beings were cut from the original images and reshaped to images with 32x32 resolution, which were labeled as “10”. Other 3500 images without human bodies were cut from other parts of the images, which were labeled as “01”. These 7000 images were transferred to grayscale, then normalized to the range from 0 to 1. All the image data for training the model was stored as 32-bit float points in the hard disk. When training the model, the data were loaded by the Python program. After reshape and extend the dimension of data to fit the methods of TensorFlow, the data were sent to the input port of the initialized model.

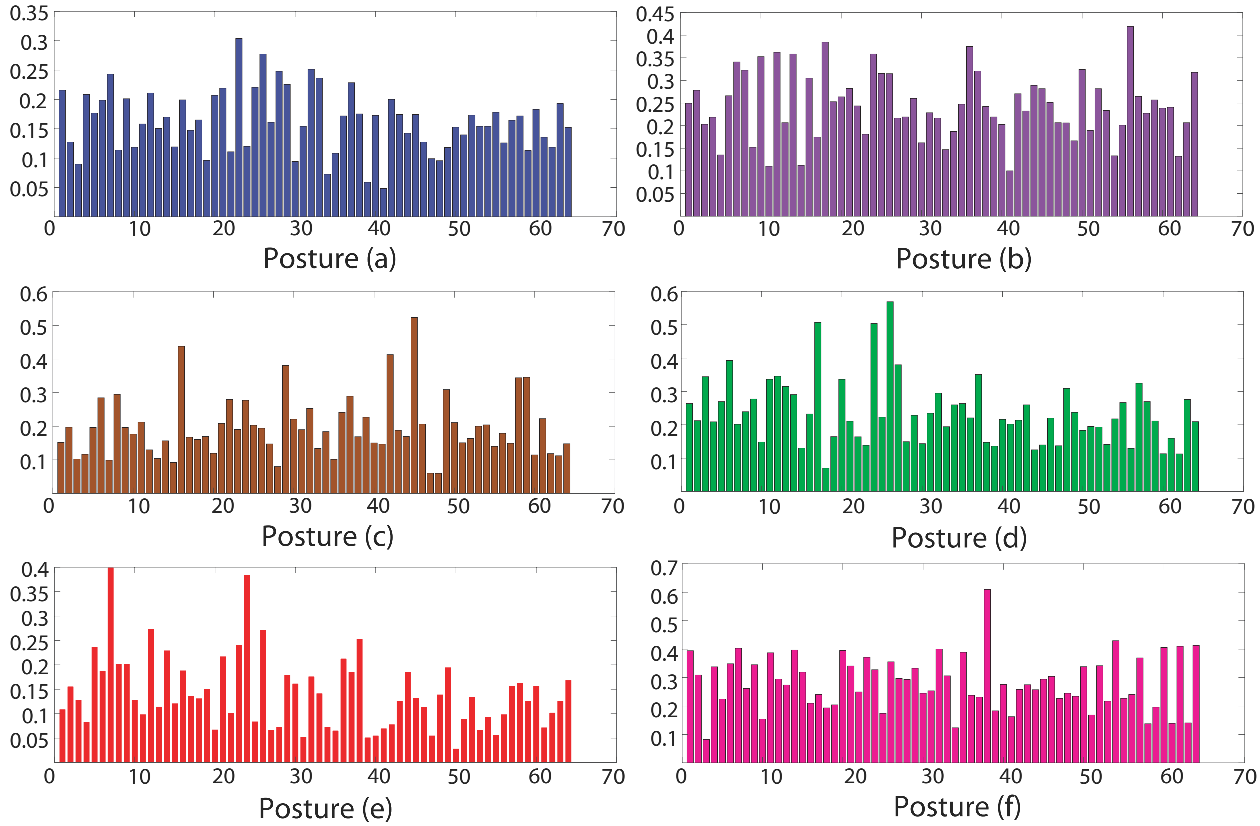

Fig. 7: Typical feature vector values for Histogram of Gradient of postures.

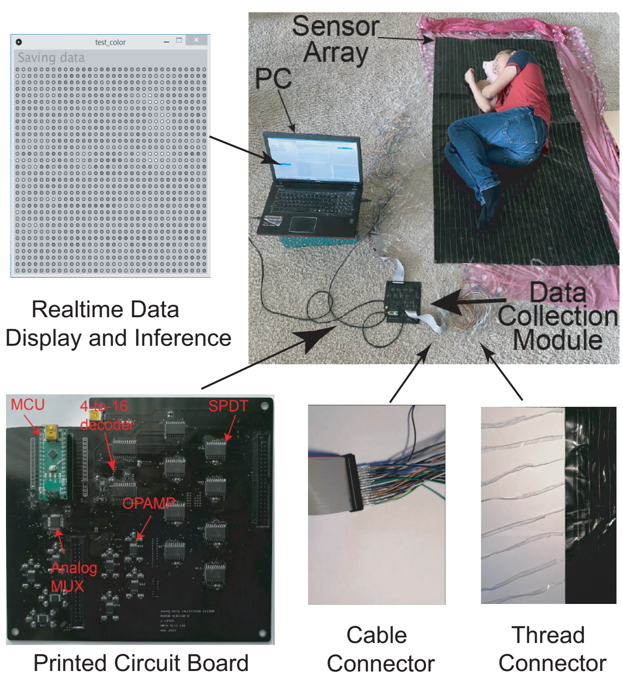

Fig. 8: System setup of the sleeping posture recognition system with realtime data display and inference interface.

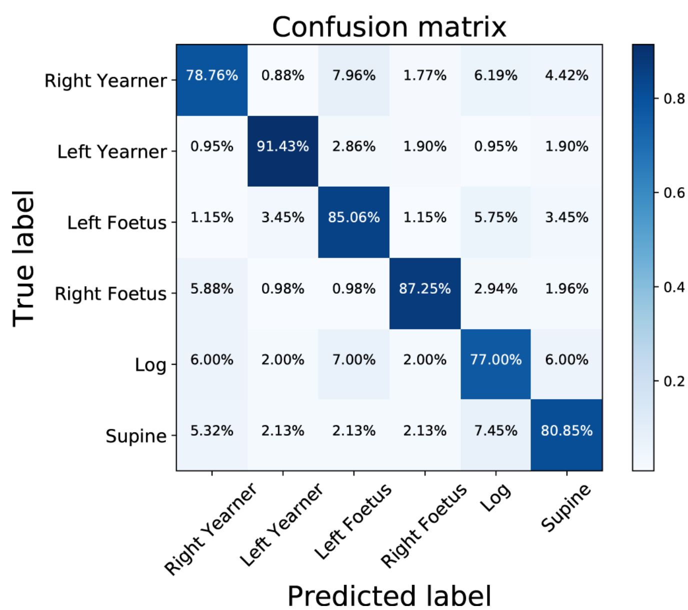

Fig. 9: Confusion matrix of the algorithm using HOG and SVM with data from all the subjects.

We collected 3005 frames of pressure data using our system for training and testing. The voltage of each node was sampled and transmitted by the data collection module with the Arduino Nano and the UART. The Python program on a PC retrieved the raw data and put the data at the corresponding position in matrices by analyzing the index of the raw data. All the data were stored as 16-bit unsigned integers in text files while the beginning and end flags are stored as strings. Each collected data sample was normalized into a value between -1 and +1 by using the minimum and the maximum values in the dataset, which accelerates the convergence of the model in the training process.

In order to perform real-time posture classification, in the inference stage, the data sampled and transmitted by the data collection module were reshaped and normalized by the Python program directly and the flags were removed. Then the processed data were sent to the model. The transient data were stored permanently in the disk. The variables of the Python program were used to store data for another cycle.

B. Real-time Display

A real-time display panel was built with the Processing programming tool. To visualize the input data in the display panel, 1024 (32x32) nodes are illustrated using grayscale. A lighter color represents a higher sampled value. All the nodes were initialed to 0 which means the color is pure dark. The program uses the UART port of the PC to communicate with the Arduino Nano in the data collection module. The program starts to store data when a flag of the frame beginning is recognized. When the flag of the frame end is detected, the data are reshaped to a 32x32 data array to the display panel. A multi-thread technique was applied so that the data retrieving and display functions can run simultaneously. The refresh rate of the display was the same as the data collection rate. The data received by this program will not be stored in the hard disk. This program facilitates the analysis of the frame region which contains the pixel information of the subject. It also checks the status of the sensors. The interface of the real-time display module is shown in Fig.8.

IV. EXPERIMENT RESULTS

By applying transfer learning, both the feature extractor and the classifier were trained. All the training, testing, and inferencing process were run on a PC using TensorFlow 2.0. Compared with the high accuracy of CNN with transfer learning, the algorithm of HOG and SVM achieves an accuracy of 83.36% with the data from all the participants without transfer learning. The confusion matrix is shown in Fig.9.

A. CNN Feature Extractor

The CNN feature extractor in this work is the first two 2-Dimensional convolutional layers of the model trained with data from the MPII dataset. The input of the model is a frame of a grayscale image with a size of 32x32 while the output is the classification result encoded with a 2-bit binary code. The batch size is 20 and the initial learning rate is 0.01 with a decay_rate of 0.7 for every 350 iterations. The epoch number is 1. The optimizer is set as Adam and the cross entropy is used as loss function, the accuracy reaches 86.94% with loss decreases to 0.3490. The training speed is 950 us/sample.

B. Classifier

After cutting the fully connected layers, the feature extractor was attached with two new fully connected layers acting as the classifier for sleeping posture recognition. The input of the new model is the same as the feature extractor but the output is the

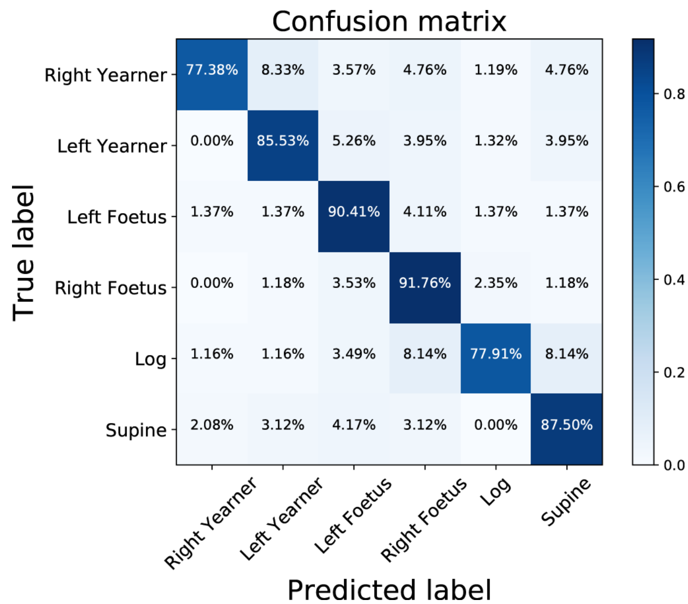

Fig. 10: Confusion matrix using the CNN model (without transfer learning) with data from all the subjects.

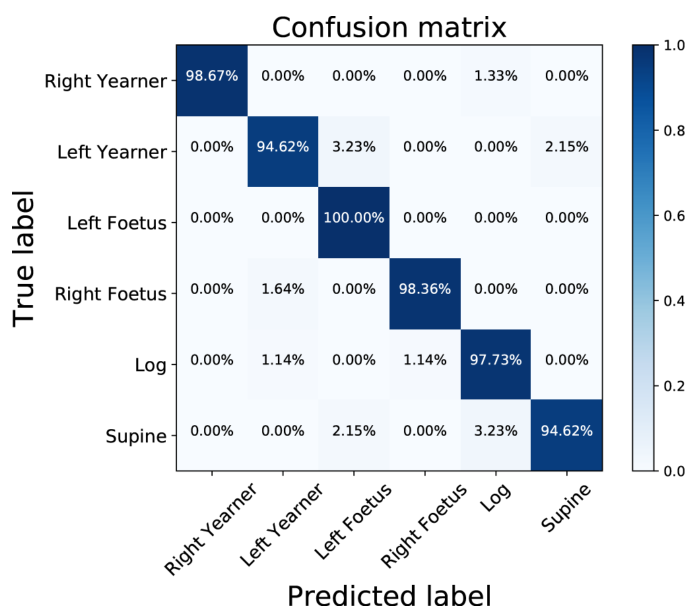

Fig. 11: Confusion matrix with the transfer learning model from the subject (1).

6-bit one-hot binary code that represents 6 sleeping postures. Shallow data were collected. Transfer learning was applied to improve performance and avoid overfitting. We implemented two testing methods, the first is normal training-testing and the second is subject-specific training-testing. We analyzed the performance of feature extraction and classification using both testing methods.

In the normal training-test method, 70% of the collected data were used to train the model while the other 30% was used to test the model. Data were randomly selected. The batch size is set as 10 and the initial learning rate is set as 0.03 with decay rate as 0.75 for every 200 iterations. The number of epoch is 10. This method achieves the accuracy of 84.80% with loss decreases to 0.8424 and the training speed of 338

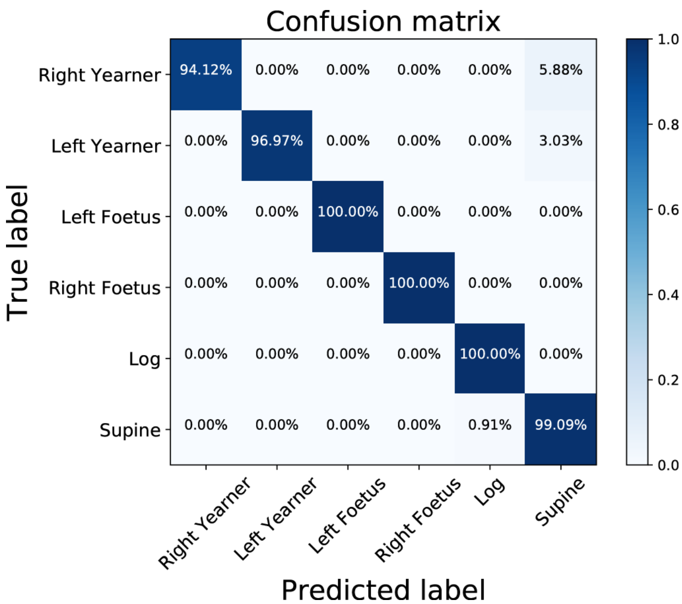

Fig. 12: Confusion matrix with the transfer learning model from the subject (2).

us/sample.

In the subject-specific method, 20% of data from the individual participant is used to training the model and the other 80% of the data is used to test the model. The data selection is also random. The batch size is set as 10 and the learning rate is 0.03 without decay. The number of epoch is also 10. The accuracy of this method is shown in the table. The confusion matrices for the testing results of models trained with participants 1∼5 is shown in Fig.11 ∼ Fig.15 respectively.

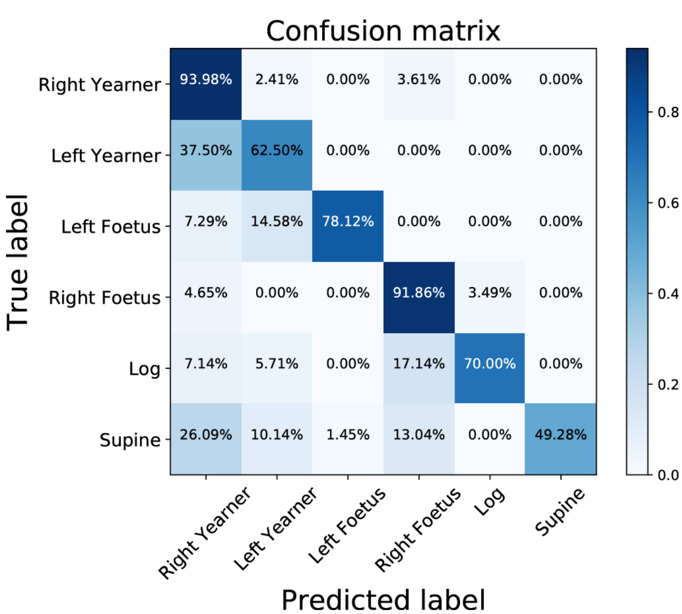

Fig. 13: Confusion matrix with the transfer learning model from the subject (3).

V. Discussion

Compared with other similar sleep posture recognition systems using pressure sensors, the main advantages of the

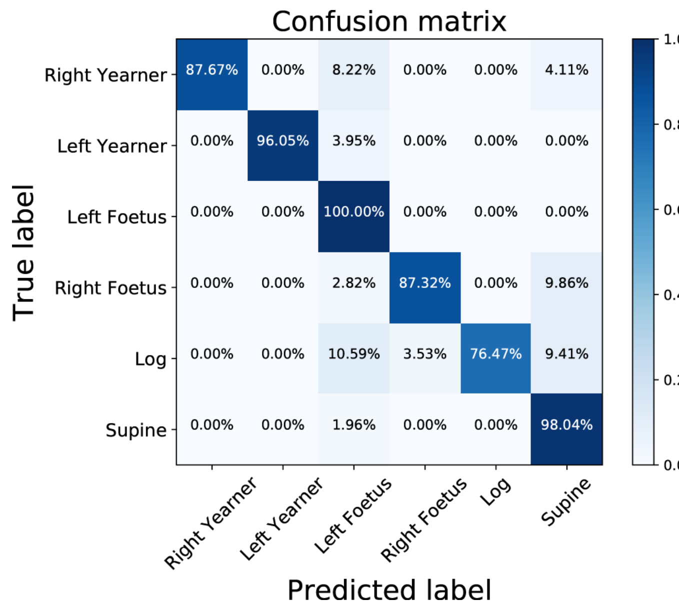

Fig. 14: Confusion matrix with the transfer learning model from the subject (4).

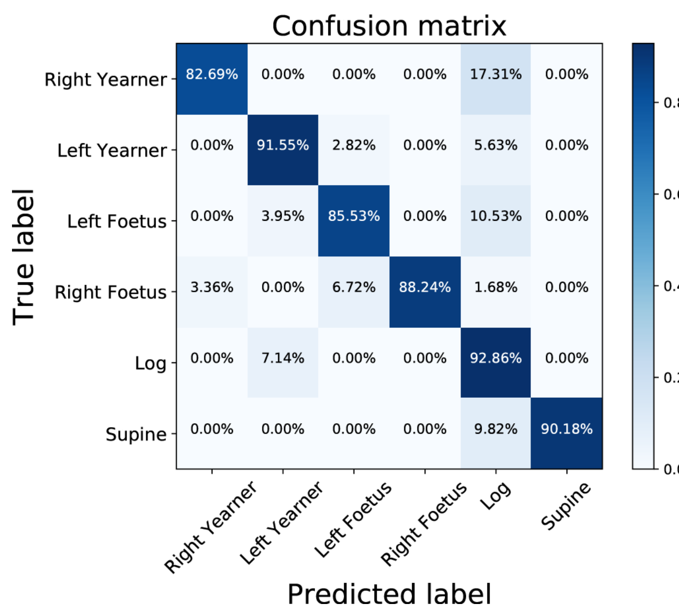

Fig. 15: Confusion matrix with the transfer learning model from the subject (5).

proposed system are the low-cost bedsheet and thin thickness. The proposed system uses conductive threads and the pressure-sensitive conductive sheet. The 11-inch by 11-inch pressure-sensitive conductive sheet costs \$5, which equals to \$0.0064/cm^2. The Stainless Thin Conductive Thread 2-ply roll costs \$7/23 meters, which equals to \$0.304/meter. This is equivalent to \$130 for the whole sensing bedsheet: \$103.7 for the sheet and \$26.3 for the threads. Other similar systems usually use commercial FSR sensor arrays, which are apparently more expensive, the market price of FSR is \$7. To make a 1024 sensor array for the whole bedsheet it would cost \$7168. Another advantage of the pressure-sensitive conductive sheet is that it is light weighted and easy to carry.

TABLE I: Accuracy and Inference Speed of the participants.

Data of Participant	Accuracy	Loss	Speed (us)
(1)	97.20%	0.2265	354
(2)	98.60%	0.084	354
(3)	80.20%	0.7373	347
(4)	91.40%	0.3785	350
(5)	88.80%	0.4118	434
summary (m+s)	91.24% $\pm$ 7.37%	0.377 $\pm$ 0.245	367.8 $\pm$ 37.124

The thickness of the pressure-sensitive conductive sheet in our system is only 0.1mm while the thickness of commercial FSR sensors is usually between 0.2-1.2 mm. Therefore patients can use our proposed system at home or even during travel. This is also very helpful for keeping the patient at home for remote monitoring.

The cost of using the pressure-sensitive conductive sheet is that the resistance between the conductive threads across the pressure-sensitive conductive sheet brings instability, which may decrease the recognition accuracy. This brings more challenges in signal processing. For example, the classification accuracy is a little bit lower than the FSR based sensing systems. To alleviate the problem from hardware, we introduced the transfer learning-based subject-specific classification to compensate for the accuracy loss. This method may require a few times of calibration and training with the individual data from a specific subject. To obtain the data, the subject-specific recognition can be done by a calibration process to let the subject lay down with certain postures before the real recognition starts in order to collect subject-specific data for the transfer learning model. This would take a few extra minutes once a new patient is using the system for the first time. We think this is feasible. Another drawback is that by doing this the system needs the training data from the subject before it could conduct inference. This means that the system would not perform inference for a completely new subject. The idea of applying subject-specific training and transfer learning is to improve the success rate in order to compensate for the uncertainty introduced by the low complexity sensing system. The system is not using a general set of model parameters. This paper focuses on system integration. The main contribution is to apply the transfer learning algorithm in the system but not proposing a new algorithm or modifying the existing algorithms. In summary, to balance trade-offs between accuracy, cost, and complexity of data collection procedures, the choice of using different types of sensors depends on the specific medical applications and cost considerations.

Another important feature of the system is real-time processing. Compared to other similar systems, the data collection module in our system provides real-time data communication between sensors and machine learning systems. Real-time inference results may help patients with serious sleep disorders such as sleep apnea. By introducing subject-specific transfer learning and real-time processing, the system also has the potential to combine the instant recorded data and historical patient data to perform better analysis to find the abnormality of the sleeping posture, which may help in early detection of health problems and introduce early intervention.

In the future, real-time processing can also be achieved using temporal difference, spatial difference, or address-event representation (AER) methods in image sensing to further reduce processing complexity and system power. Other kinematics modeling methods such as Simultaneous Localization and Mapping (SLAM), which is popular in Robotics, could also be applied in the sleep posture recognition application. It is also possible to integrate a wireless link into the system to replace the cable. The current system has known limitations as other systems, for example serving the patient with an amputation. However, the subject-specific training may compensate for this shortcoming. The low complexity sensor-learning architecture has the potential to be implemented on hardware, such as an FPGA, to further reduce the system cost and improve the privacy protections of the patient [13]. We are currently working on converting the smart bedsheet system into a local processing block to avoid using a computer.

VI. Conclusion

In this work, a real-time low-cost sleeping posture recognition system with high performance and privacy was implemented. The system used transfer learning to obtain high accuracy with shallow data and avoid overfitting. The model has a relatively simple structure and been tested using both normal training-testing and subject-specific testing methods. The system provides a low complexity solution for real-time sleeping posture recognition. The computation of the model includes multiply-accumulation operation with activation functions as ReLU and Hyperbolic tangent. The system has the potential to be implemented on hardware in the future.

References

[1] F. Lorussi, W. Rocchia, E. P. Scilingo, A. Tognetti, and D. De Rossi, “Wearable, redundant fabric-based sensor arrays for reconstruction of body segment posture,” *IEEE Sensors Journal*, vol. 4, no. 6, pp. 807–818, 2004.

[2] R. Paradiso, G. Loriga, and N. Taccini, “A wearable health care system based on knitted integrated sensors,” *IEEE Transactions on Information Technology in Biomedicine*, vol. 9, no. 3, pp. 337–344, 2005.

[3] A. Pantelopoulos and N. G. Bourbakis, “A survey on wearable sensor-based systems for health monitoring and prognosis,” *IEEE Transactions on Systems, Man, and Cybernetics, Part C (Applications and Reviews)*, vol. 40, no. 1, pp. 1–12, 2010.

[4] H. H. Asada, P. Shaltis, A. Reisner, Sokwoo Rhee, and R. C. Hutchinson, “Mobile monitoring with wearable photoplethysmographic biosensors,” *IEEE Engineering in Medicine and Biology Magazine*, vol. 22, no. 3, pp. 28–40, 2003.

[5] G. Unguez, C. Duran, D. Valles-Rosales, M. Harris, E. Salazar, M. McDowell, and W. Tang, “3d-printed wearable backpack stimulator for chronic in vivo aquatic stimulation,” in *Engineering in Medicine and Biology Society (EMBC), 2015 37th Annual International Conference of the IEEE*, Aug 2015, pp. 2147–2150.

[6] X. Tang, Q. Hu, and W. Tang, “Delta Sigma Encoder for Low-Power Wireless Bio-Sensors Using Ultrawideband Impulse Radio,” *IEEE Transactions on Circuits and Systems II: Express Briefs*, vol. 64, no. 7, pp. 747–751, 2017.

[7] W. Tang, P. M. Furth, V. H. Nammi, G. Panwar, V. Ibarra, X. Tang, G. A. Unguez, and S. Misra, “An aquatic wireless biosensor for electric organ discharge with an integrated analog front end,” *IEEE Sensors Journal*, vol. 19, no. 15, pp. 6260–6269, 2019.

[8] T. Harada, T. Sato, and T. Mori, “Estimation of bed-ridden human’s gross and slight movement based on pressure sensors distribution bed,” in *Proceedings 2002 IEEE International Conference on Robotics and Automation (Cat. No.02CH37292)*, vol. 4, 2002, pp. 3795–3800 vol.4.

TABLE II: Comparison between this work and recent published references.

	Sensor Hardware		Processing Algorithm		System Specification		
Method	Sensor Type	Number of Sensors	Feature Extraction	Learning Method	Number of Postures	Processing time or rate	Accuracy Rate
This method	Pressure Sensitive Sheet	32x32 =1024	HOG	SVM	6	<400 ms (Sampling and Processing)	86.94%
			CNN				84.80%
			CNN with Transfer Learning				91.24%
Mater et al., 2020 [28]	FSR sensors	64x27 =1728	HOG + LBP	FFANN	4	N/A	97%
Enokibori et al., 2018 [29]	FSR sensors	3200	No feature extraction	Deep Neural Network	3	N/A	99.7%
Huang et al., 2017 [30]	FSR sensors	360	Resistance Values	Scale and Moving Average Window	3	1 Hz (Sampling and Processing)	87% and 96%
Heydarzadeh et al., 2016 [31]	FSR Sensors	32x64 =2048	HOG	Deep Neural Network	3	1.7 Hz (Sampling) 10 ms (Processing)	98.1%
Xu et al., 2016 [32]	Pressure Sensor	64x128 =8192	Body-Earth Mover's Distance	K-nearest Neighborhood	14	<5 mins (Sampling and Processing)	91.21%
Xu et al., 2015 [35]	Pressure Sensor	64x128 =8192	Projection of Pressure Distribution	K-nearest Neighborhood	6	N/A	90.6%
Mineharu et al., 2015 [36]	Pressure Sensor	34x52 =1768	Spatial features	Support Vector Machine	9	N/A	77.14%
Baran et al., 2013 [37]	Pressure Sensor	2048	Posture Binary Signature	K-nearest neighborhood	8	60 ms (Processing only)	97.1%
Liu et al., 2014 [38]	3-layer eTextile FSR	8192	Spatial and Body Part Features	Minimum Class Residual Classifier	6	210 ms (Processing only)	83.07%
Huang et al., 2014 [39]	Piezoelectric Polymer	64x128 =8192	Local Linear Embedding and Isomap with k-Nearest Neighbor Searching		5	N/A	Avg 90.3%
Metsis et al., 2011 [41]	Pressure Sensors	32X32 =1024	Pressure Image Central Moments	PCA+HMM	3	N/A	90.4%
Hsia et al., 2009 [43]	FSR Sensors	56	Kurtosis and Skeweness of Pressure Map	Bayesian and PCA+SVM	6	N/A	81% and 85%
Hsia et al, 2008 [44]	FSR Sensors	16	Kurtosis and Skeweness of Pressure Map	Bayes	3	N/A	78.7%

[9] A. Arcelus, C. L. Herry, R. A. Goubran, F. Knoefel, H. Sveistrup, and M. Bilodeau, "Determination of sit-to-stand transfer duration using bed and floor pressure sequences," *IEEE Transactions on Biomedical Engineering*, vol. 56, no. 10, pp. 2485–2492, 2009.

[10] F. Lorussi, E. P. Scilingo, A. Tesconi, A. Tognetti, and D. De Rossi, "Wearable sensing garment for posture detection, rehabilitation and telemedicine," in *4th International IEEE EMBS Special Topic Conference on Information Technology Applications in Biomedicine, 2003.*, 2003, pp. 287–290.

[11] X. Tang, Q. Hu, and W. Tang, "A real-time qrs detection system with pr/rt interval and st segment measurements for wearable ecg sensors using parallel delta modulators," *IEEE Transactions on Biomedical Circuits and Systems*, vol. 12, no. 4, pp. 751–761, 2018.

[12] X. Tang, Z. Ma, Q. Hu, and W. Tang, "A real-time arrhythmia heartbeats classification algorithm using parallel delta modulations and rotated linear-kernel support vector machines," *IEEE Transactions on Biomedical Engineering*, vol. 67, no. 4, pp. 978–986, 2020.

[13] Q. Hu, X. Tang, and W. Tang, "A smart chair sitting posture recognition system using flex sensors and fpga implemented artificial neural network," *IEEE Sensors Journal*, vol. 20, no. 14, pp. 8007–8016, 2020.

[14] S. Mukherjee, S. R. Patel, S. N. Kales, N. T. Ayas, K. P. Strohl, D. Gozal, and A. Malhotra, "An official american thoracic society statement: the importance of healthy sleep. recommendations and future priorities," *American journal of respiratory and critical care medicine*, vol. 191, no. 12, pp. 1450–1458, 2015.

[15] Bjarki, *7 time consuming things an average Joe spends on in a lifetime*, September 05 2013. [Online]. Available: https://www.tempo.io/blog/7-time-consuming-things-an-average-joe-spends-in-a-lifetime#:~:text=A%20good%20night's%20sleep%20is,one%20third%20of%20their%20life.

[16] N. B. Kavey, A. Blitzer, S. Gidro-Frank, and K. Korstanje, "Sleeping position and sleep apnea syndrome," *American journal of otolaryngology*, vol. 6, no. 5, pp. 373–377, 1985.

[17] G. Mills and A. Chaffe, "Sleeping positions adopted by pregnant women of more than 30 weeks gestation," *Anaesthesia*, vol. 49, no. 3, pp. 249–250, 1994.

[18] K. N. Kim, J. W. Jeoung, K. H. Park, D. M. Kim, and R. Ritch, "Relationship between preferred sleeping position and asymmetric visual field loss in open-angle glaucoma patients," *American journal of ophthalmology*, vol. 157, no. 3, pp. 739–745, 2014.

[19] C. Gorecki, S. J. Closs, J. Nixon, and M. Briggs, "Patient-reported pressure ulcer pain: a mixed-methods systematic review," *Journal of pain and symptom management*, vol. 42, no. 3, pp. 443–459, 2011.

[20] J. A. Oulton, "The global nursing shortage: An overview of issues and actions," *Policy, Politics, & Nursing Practice*, vol. 7, no. 3_suppl, pp. 34S–39S, 2006, pMID: 17071693. [Online]. Available: https://doi.org/10.1177/1527154406293968

[21] S. Jeon, T. Park, A. Paul, Y.-S. Lee, and S. Son, "A wearable sleep position tracking system based on dynamic state transition framework," *IEEE Access*, vol. PP, pp. 1–1, 09 2019.

[22] P. Jiang and R. Zhu, "Dual tri-axis accelerometers for monitoring physiological parameters of human body in sleep," in *2016 IEEE SENSORS*, 2016, pp. 1–3.

[23] P. Jeng and L. Wang, "An accurate, low-cost, easy-to-use sleep posture monitoring system," in *2017 International Conference on Applied System Innovation (ICASI)*, 2017, pp. 903–905.

[24] S. Liu and S. Ostadabbas, "Seeing under the cover: A physics guided learning approach for in-bed pose estimation," *22nd International Conference on Medical Image Computing and Computer Assisted Intervention (MICCAI2019), Shenzhen, China. arXiv preprint arXiv:1907.02161*, 2019.

[25] F. Deng, J. Dong, X. Wang, Y. Fang, Y. Liu, Z. Yu, J. Liu, and F. Chen, "Design and implementation of a noncontact sleep monitoring system using infrared cameras and motion sensor," *IEEE Transactions on Instrumentation and Measurement*, vol. 67, no. 7, pp. 1555–1563, 2018.

[26] N. Mohsin, X. Liu, and S. Payandeh, "Signal processing techniques for natural sleep posture estimation using depth data," in *2016 IEEE 7th*

Annual Information Technology, Electronics and Mobile Communication Conference (IEMCON), 2016, pp. 1–8.
[27] J. Bell, *From smart pyjamas to a bedside monitor - six innovative devices for at-home sleep monitoring*, 19 Nov 2019. [Online]. Available: https://www.nsmedicaldevices.com/analysis/home-sleep-monitor/
[28] G. Matar, J. Lina, and G. Kaddoum, "Artificial Neural Network for in-Bed Posture Classification Using Bed-Sheet Pressure Sensors," *IEEE Journal of Biomedical and Health Informatics*, vol. 24, no. 1, pp. 101–110, 2020.
[29] Y. Enokibori and K. Mase, "Data augmentation to build high performance dnn for in-bed posture classification," *J. Inf. Process.*, vol. 26, pp. 718–727, 2018.
[30] Y.-F. Huang, Y.-H. Hsu, C.-C. Chang, S.-H. Liu, C.-C. Wei, T.-Y. Yao, and C.-B. Lin, "An improved sleep posture recognition based on force sensing resistors," in *Asian Conference on Intelligent Information and Database Systems*, 2017, pp. 318–3.
[31] M. Heydarzadeh, M. Nourani, and S. Ostadabbas, "In-bed posture classification using deep autoencoders," in *2016 38th Annual International Conference of the IEEE Engineering in Medicine and Biology Society (EMBC)*, 2016, pp. 3839–3842.
[32] X. Xu, F. Lin, A. Wang, Y. Hu, M. Huang, and W. Xu, "Body-earth movers distance: A matching-based approach for sleep posture recognition," *IEEE Transactions on Biomedical Circuits and Systems*, vol. 10, no. 5, pp. 1023–1035, 2016.
[33] M. Sarrafzadeh, W. Xu, M.-C. Huang, and J. J. Liu, "On-bed monitoring system for range of motion exercise with a pressure sensitive bed sheet," US Patent 9,330,342 B2, 2016.
[34] M. Sarrafzadeh, W. Xu, M.-C. Huang, N. Raut, and B. Yadegar, "Fabric-based pressure sensor arrays and methods for data analysis," US Patent 9.271,665 B2, 2016.
[35] X. Xu, F. Lin, A. Wang, C. Song, Y. Hu, and W. Xu, "On-bed sleep posture recognition based on body-earth mover's distance," in *2015 IEEE Biomedical Circuits and Systems Conference (BioCAS)*, 2015, pp. 1–4.
[36] A. Mineharu, N. Kuwahara, and K. Morimoto, "A study of automatic classification of sleeping position by a pressure-sensitive sensor," in *Proc. Int. Conf. Inform., Electron. Vis.*, 2015, pp. 1–5.
[37] M. B. Pouyan, S. Ostadabbas, M. Farshbaf, R. Yousefi, M. Nourani, and M. D. M. Pompeo, "Continuous eight-posture classification for bed-bound patients," in *Proc. 6th Int. Conf. Biomed. Eng. Inform.*, 2013, pp. 121–126.
[38] J. J. Liu, W. Xu, M.-C. Huang, N. Alshurafa, M. Sarrafzadeh, N. Raut, and B. Yadegar, "Sleep posture analysis using a dense pressure sensitive bedsheet," *Pervasive and Mobile Computing*, vol. 10, pp. 34–50, 2014.
[39] M. Huang, J. J. Liu, W. Xu, N. Alshurafa, X. Zhang, and M. Sarrafzadeh, "Using pressure map sequences for recognition of on bed rehabilitation exercises," *IEEE Journal of Biomedical and Health Informatics*, vol. 18, no. 2, pp. 411–418, 2014.
[40] S. Ostadabbas, M. Baran Pouyan, M. Nourani, and N. Kehtarnavaz, "In-bed posture classification and limb identification," in *2014 IEEE Biomedical Circuits and Systems Conference (BioCAS) Proceedings*, 2014, pp. 133–136.
[41] V. Metsis, G. Galatas, A. Papangelis, D. Kosmopoulos, and F. Makedon, "Recognition of sleep patterns using a bed pressure mat," in *Proc. 4th Int. Conf. Pervasive Technol. Related Assistive Environ.*, 2011.
[42] R. Yousefi, S. Ostadabbas, M. Faezipour, M. Farshbaf, M. Nourani, L. Tamil, and M. Pompeo, "Bed posture classification for pressure ulcer prevention," in *2011 Annual International Conference of the IEEE Engineering in Medicine and Biology Society*, 2011, pp. 7175–7178.
[43] C.C.Hsia, K.J.Liou, A.P.W.Aung, V.Foo, W.Huang, and J.Biswas, "Analysis and comparison of sleeping posture classification methods using pressure sensitive bed system," in *Proc. Annu. Int. Conf. IEEE Eng. Med. Biol. Soc.*, 2009, pp. 6131–6134.
[44] C.-C.Hsia, Y.-W.Hung, Y.-H.Chiu, and C.-H.Kang, "Bayesian classification for bed posture detection based on kurtosis and skewness estimation," in *Proc. 10th Int. Conf. e-Health Netw., Appl. Services*, 2008, pp. 165–168.
[45] "Mpii human pose dataset," http://human-pose.mpi-inf.mpg.de/.
[46] S. Sundaram, P. Kellnhofer, Y. Li, J.-Y. Zhu, A. torralba, and W. Matusik, "Learning the signatures of the human grasp using ascalable tactile glove," *Nature*, vol. 569, pp. 698–702, 2019.
[47] S. J. Pan and Q. Yang, "A survey on transfer learning," *IEEE Transactions on Knowledge and Data Engineering*, vol. 22, no. 10, pp. 1345–1359, 2010.

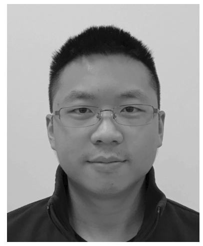

Qisong Hu (S'17) received the Bachelor of Engineering degree from the University of Electronic Science and Technology of China, Chengdu, China, in 2013 and PhD. degree in Electrical and Computer Engineering from New Mexico State University, Las Cruces, NM, USA, in 2020. He joined the ASIC group of Maxlinear INC, Carlsbad, CA, USA, in 2020. He has been engaged in the design of High-Speed Interconnects.

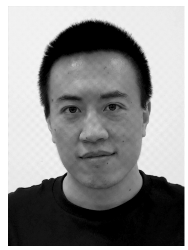

Xiaochen Tang (S'17) received the B.E. degree in electronics science and technology and the M.E. degree in microelectronics and solid-state electronics from the Harbin Institute of Technology, Harbin, China, in 2010 and 2012, respectively, and the Ph.D. degree in electrical engineering from New Mexico State University, Las Cruces, USA, in 2020. He is currently a post doc researcher in Texas A&M University, College Station, TX, USA. His research interests include low-power biomedical integrated circuits and wearable biomedical devices.

Wei Tang (S'06-M'12) received the B.Sc. degree in microelectronics from Peking University, Beijing, China, in 2006, and the Ph.D. degree in electrical engineering from Yale University, New Haven, CT, USA, in 2012. He joined the Klipsch School of Electrical and Computer Engineering, New Mexico State University, Las Cruces, NM, USA, as an Assistant Professor in 2012 and was promoted to an Associate Professor in 2018. He is currently an Associate Professor with the Klipsch School of Electrical and Computer Engineering, New Mexico State University. His research interests include low-power analog/mixed-signal/digital/RF integrated circuits design and implementation, hardware-friendly digital signal processing and image processing algorithms, and biomedical sensors and wearable devices, circuits and systems. He was a recipient of the National Science Foundation Faculty Early Career Award in 2017 and currently holds the Paul W. and Valerie Klipsch Distinguished Professorship of New Mexico State University.